Article

High Dispersion of Platinum Nanoparticles over Functionalized Zirconia for Effective Transformation of Levulinic Acid to Alkyl Levulinate Biofuel Additives in the Vapor Phase

Ramyakrishna Pothu [1,*], **Naresh Mameda** [2], **Harisekhar Mitta** [3], **Rajender Boddula** [4,5,*], **Raveendra Gundeboyina** [6], **Vijayanand Perugopu** [4], **Ahmed Bahgat Radwan** [5], **Aboubakr M. Abdullah** [5] **and Noora Al-Qahtani** [5,*]

1 School of Physics and Electronics, College of Chemistry and Chemical Engineering, Hunan University, Changsha 410082, China
2 Department of Engineering Chemistry, College of Engineering, Koneru Lakshmaih Education Foundation, Vaddeswaram 520002, India
3 Laboratory of Chemical Technologies, Ghent University, 9052 Zwaijnarde, Belgium
4 Energy & Environmental Engineering Department, CSIR−Indian Institute of Chemical Technology, Hyderabad 500007, India
5 Center for Advanced Materials (CAM), Qatar University, Doha 2713, Qatar
6 Department of Process and Plant Technology, Brandenburg University of Technology, 03046 Cottbus, Germany
* Correspondence: research.ramyakrishna@gmail.com (R.P.); research.raaj@gmail.com (R.B.); noora.alqahtani@qu.edu.qa (N.A.-Q.)

Abstract: In recent years, functionalized metal oxides have been gaining popularity for biomass conversion to fuels and chemicals due to the global energy crisis. This study reports a novel catalyst based on noble metal immobilization on functionalized zirconia that has been successfully used in the production of biofuel alkyl levulinates (ALs) from lignocellulosic biomass-derived levulinic acid (LA) under vapor-phase. The wet impregnation method was used to immobilize Pt-metal nanoparticles on zirconia-based supports (silicotungstic acid zirconia, STA-ZrO$_2$; sulfated zirconia, S-ZrO$_2$; and tetragonal zirconia, t-ZrO$_2$). A variety of physicochemical techniques were used to characterize the prepared catalysts, and these were tested under atmospheric pressure in continuous flow esterification of LA. The order of catalytic activity followed when ethyl levulinate was produced from levulinic acid via esterification: Pt/STA-ZrO$_2$ ≫ Pt/S-ZrO$_2$ ≫ Pt/t-ZrO$_2$. Moreover, it was found that ALs synthesis from LA with different alcohols utilizing Pt/STA-ZrO$_2$ catalyst followed the order ethyl levulinate ≫ methyl levulinate ≫ propyl levulinate≫ butyl levulinate. This work outlines an excellent approach to designing efficient catalysts for biofuels and value-added compounds made from biomass.

Keywords: alkyl levulinates; biofuels; functionalized zirconia; batch processes; bifunctional catalysts

1. Introduction

The development of biofuels and chemicals using renewable energy sources to replace petroleum-based oil reserves as received much interest in the recent decade due to its attractive environmental impact and growing energy consumption in society [1,2]. Levulinic acid (LA) is one of the top 12 biomass-derived platform chemicals that are recommended by the US Department of Energy (DOE) and the National Renewable Energy Laboratory (NREL) [3]. It can be turned into chemicals and fuels with additional value, such as alkyl levulinate (ALs) and γ-valero lactone (GVL), as well as acrylic acid, succinic acid, diphenolic acids, amino levulinic acids, valeric acid (VA), and 2-methyltetrahydrofuran (MTHF) [4]. ALs are used as raw ingredients in biofuels, biodiesel blends, plasticizers, fragrances, green solvents, chemicals, and drugs, etc. [5,6]. Among ALs, ethyl levulinate

(EL) is an essential LA ester and is widely used as economically viable biodiesel and bio-fuel additive. EL production from LA utilizing the development of catalytic technology under mild reaction circumstances is a promising method compared to any other raw materials (5-hydroxymethylfurfural, 5-ethoxymethylfurfural) [7–9]. As a result, many different catalytic techniques for producing EL from LA (homogeneous and heterogeneous catalysis) have been reported. Mineral acids (HCl, H_3PO_4, and H_2SO_4) [6–8] and ionic liquids ([BMlm-SH] [HSO_4]) [10] produced remarkable findings. Still, they have significant problems with catalytic poisoning. Corroded equipment seems to be slow in separation, and purification procedures require a neutralization phase and non-recoverable catalyst, making them inappropriate for practical applications [11]. These faults can be overcome with heterogeneous solid acid catalysts, which are the ideal alternative to homogeneous catalysts since they are easier to recover, separate from reaction products, perform more reactions, and reduce environmental impact [12–14].

Functionalized zirconia-based catalyst systems, such as sulfated (S) zirconia and silico-tungstic acid (STA) zirconia, have received a great deal of interest as solid acid catalytic support because they provide a lot of flexibility in regards to both acidity and basicity, as well as remarkable stability and availability of active sites on the surface [15]. Doping zirconia with other oxyanions may improve catalytic performance in reactions such as heavy-oil upgrading [16], n-butane isomerization [17], phenethoxybenzene to aromatic hydrocarbons conversion [18], and biofuel synthesis [19]. Functionalized ZrO_2 catalysts have been described as efficient catalysts for biomass conversions [15,20,21]. Derya et al. have developed a sulphated zirconia-loaded hydroxyethyl cellulose catalytic membrane for esterification of LA with ethanol resulted 89% of LA conversion [22]. Saravanamurugan et al. investigated EL (13%) synthesis from glucose by the SO_4^{2-}/ZrO_2 catalyst at 140 °C for 24 h [23]. Under similar conditions, Morales et al. SO_4^{2-}/ZrO_2 loaded SBA-15 to 30.7% EL yield [24]. Song et al. examined the $H_3PW_{12}O_{40}$/ZrO_2 for direct alcoholysis of furfural alcohol to EL yield (70.2%) at 120 °C for 3 h [25]. Zhang et al. investigated the EL synthesis from glucose with ethanol over SO_4^{2-}/ZrO_2@Al_2O_3-3M catalyst [26], and EL yielded 37.5 mol% at 200 °C for 5 h. Quereshi et al. reported that 40 wt.% STA was loading in ZrO_2 support for LA transformation to EL yield (90 mol %) at 110 °C in 0.5 h in a microwave reactor [27]. However, several strategies and techniques have limitations, such as complex catalyst production, low catalyst stability, and expensive precursors or instrumentation. Even ultralow loading of Pt significantly increased the catalytic activity of monometallic ox-ide in the biomass conversions such as LA into GVL [28], glycerol into 1,3-propanediol [29], furfuryl alcohol into 2-methylfuran [30], etc. In fact, Pt deposition appreciably enhanced the Brønsted acidity and caused the high product yield. Therefore, the high number of Brønsted acid sites favors the removal of the hydroxyl groups from the LA, producing much more alkyl levulinates. Thus, we present here the ultralow loading of Pt-immobilized functionalized ZrO_2 catalyst recipes via the co-precipitation/impregnation method and investigated the vapor phase direct conversion of LA into ALs using a continuous fixed-bed reactor, and alcohol (methanol, ethanol, propanol and butanol) as a solvent. The physic-ochemical properties of the materials were analyzed using a variety of characterization techniques, including XRD, TEM, CO chemisorption, and BET-surface area measurements. Based on the optimal catalyst for EL synthesis, the effect of LA concentration, reaction temperature, hydrogen donor, ethanol feed, catalyst amount, and the catalyst stability on the catalyst activity were investigated.

2. Materials and Methods

2.1. Materials

Zirconium oxychloride ($ZrOCl_2 \cdot 8H_2O$), aqueous ammonia (NH_3) (25%), cetyltrimethy-lammonium chloride (CTMC), silicotungstic acid (STA), ammonium sulfate (($NH_4)_2SO_4$), chloroplatinic acid ($H_2PtCl_6 \cdot 6H_2O$), and levulinic acid (LA) were purchased from Sigma-Aldrich (St. Louis, MI, USA).

2.2. Preparation of Pt-Supported Functionalized Zirconia Catalysts

Tetragonal ZrO_2 (t-ZrO_2) support was prepared by co-precipitation and calcination. Initially, various 0.1 M aqueous solutions of $ZrOCl_2 \cdot 8H_2O$ and CTMC were prepared. After adding the CTMC solution to the $ZrOCl_2 \cdot 8H_2O$ solution, the mixture was agitated for 15 min. In order to precipitate the product, aqueous NH_3 (25%) was slowly added until a pH range of 11.5 was reached, then swirled for 1 h before leaving it in a water bath at 60 °C with constant stirring for 4 h. It was then filtered, washed with DI water and acetone until the mixture was free of surfactant, and dried at 90 °C for 20 h. The solid powder was calcined in the air at 500 °C for 2 h to produce t-ZrO_2. STA-ZrO_2 was prepared using the wet impregnation by using Keggin type STA (20 wt.%) loading on t-ZrO_2 support. Initially, STA and ZrO_2 were first measured and dissolved individually in 10 mL and 100 mL distilled H_2O. STA was dropped dropwise to the ZrO_2 mixture, stirred, and heated at 40 °C. The resulting combination was then aged in the beaker for 24 h. The resultant mixture's precipitates were prepared by evaporating the aged solution with a rotary evaporator and then calcining at 350 °C for 3 h in a static air atmosphere. Similarly, sulphated ZrO_2 catalyst (S-ZrO_2) was also prepared by the wet impregnation method and ammonium sulfate ((NH_4)$_2SO_4$) was used as a precursor for sulphate instead of STA in the above procedure.

The co-precipitation approach was used to make Pt supported by STA-ZrO_2 (Pt/STA-ZrO_2), S-ZrO_2 (Pt/S-ZrO_2), and t-ZrO_2 (Pt/t-ZrO_2). The Pt metal loading in the catalysts was kept constant for all catalysts at 2 wt.%. A fixed quantity of metal precursors was dissolved in distilled water; then, l M $NaHCO_3$ solution was added dropwise under steady stirring until the pH of the solution was 9, and metal hydroxides precipitated. The needed amount of ZrO_2 support was also added, and the slurry was mixed for 6 h before being aged at room temperature for 12 h. The supernatant liquid was decanted after aging, and the dense slurry was rinsed with distilled water before being filtered via a vacuum filter. Finally, the filtered materials were dried at 100 °C under a vacuum furnace for 12 h, and then dried samples under calcination at 350 °C for 4 h.

2.3. Catalyst Characterization

X-ray powder diffraction (XRD) was performed on the samples using a Rigakuminiflex X-ray diffractometer apparatus with Ni-filtered Cu Kα radiation (λ = 0.l5406 nm) produced at 30 kV and 15 mA. The KBr disc approach was used at room temperature to record IR spectra on a Nicolet 670 GC-FT-IR spectrometer. The sample morphology was examined using transmission electron microscopy (TEM) in a high-resolution JEOL 2010 microscope after 1 mg of the reduced sample was sonicated for 10 min in 5 mL of methanol. The droplets were then put on a carbon membrane-shielded porous Cu grid. N_2-adsorption-desorption isotherms experiments were performed at 196 °C using Autosorb l (Quantachrome Instruments, Boynton Beach, FL, USA) and the multipoint BET method with a cross-sectional area of 0.0162 nm^2 to examine the textural characteristics. In a Micromeritics Autochem 2920 AutoChem 2920 instrument with a TCD detector, CO-chemisorption tests were conducted. Prior to adsorption, 0.1 g of the sample was reduced for 3 h at 300 °C in flowing H_2 (50 mL/min), flushed for 1 h at 300 °C in He gas, and cooled to room temperature. The stoichiometric factor (CO/Pt) was utilized to calculate Pt dispersion and average particle size, and pulses of 9.96% CO-balanced He gas were injected over the reduced samples at 300 °C at regular intervals to measure CO uptake.

2.4. Catalytic Activity Studies

The esterification of LA with alcohol was carried out under atmospheric pressure in a fixed-bed quartz downflow reactor (42 cm long, 12 mm i.d.). In a typical catalytic run, 0.4 g of precisely weighed catalyst material was added to the reactor along with the same weight of glass beads and held by ends of glass wool. Ceramic wool was placed above the catalyst bed to prevent reactants from coming into contact with it. A B-Braun syringe pump was used to inject the reactant (a combination of LA and ethanol), which was then

vaporized for one hour at 300 °C in a preheating zone on top of the catalyst bed. A flame ionization detector and an HP-l capillary column (0.25 mm i.d., l5 m long) were used with a gas chromatograph HP-6890 to analyze the mixture of reaction products at regular intervals. The CHNS analyzer elementar Vario micro cube model was used to estimate the amount of carbon in the catalysts that were used. The steady state mass carbon balance was found to be more than 97.2%. To calculate the conversion of LA and the selectivity of desired products, the following formulas were utilized.

$$\text{LA conversion (\%)} = \frac{\text{mole of LA (in)} - \text{moles of LA (out)}}{\text{Moles of LA in the feed (in)}} \times 100 \qquad (1)$$

$$\text{Product selectivity (\%)} = \frac{\text{Moles of one product}}{\text{moles of all products}} \times 100 \qquad (2)$$

3. Results and Discussion

3.1. X-ray Diffraction (XRD) Analysis

Figure 1 shows the XRD patterns of the tetragonal and functionalized zirconia supported Pt catalysts. The observed high-intensity diffraction peaks at 30.6, 50.4, and 60.1° are assigned to the (101), (112), and 211) planes typical of t-ZrO_2 (JCPDS Card 79–1764). The other four small diffraction peaks with relatively low intensities at 2θ = 39.6, 47.4, and 67.1°, which are assigned to the (111), (200), and (220) planes, respectively, are consistent with the face-centered cubic structure of Pt (JCPDS Card 04-0802), thus indicating the presence of crystalline Pt immobilized on the surface of functionalized and tetragonal zirconia catalysts [31]. The relatively broad and low-intensity diffraction peaks indicate the small crystalline size and loading of the Pt nanoparticles. Compared with Pt/t-ZrO_2 and Pt/S-ZrO_2, the Pt/STA-ZrO_2 sample has obtained small Pt species (Figure 1). Using each XRD peak, the average size of Pt crystallite can be computed using the width of the reflection corresponding to the Debye–Scherrer equation: the calculated crystallite sizes of all the catalysts were achieved to be 2.8 nm, 5.5 nm, and 10.6 nm.
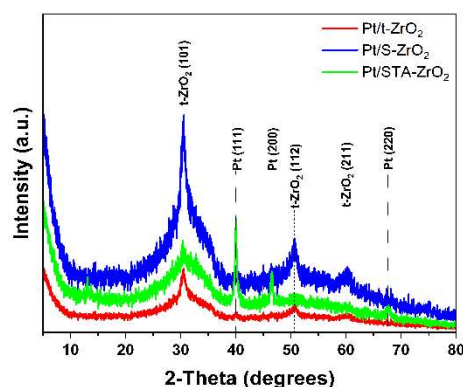

Figure 1. XRD patterns recorded for Pt immobilized functionalized zirconia materials.

3.2. Transmission Electron Microscope (TEM) Analysis

The TEM images and particle size distributions of Pt-loaded t-ZrO_2, S-ZrO_2, and STA-ZrO_2 samples are displayed in Figure 2. Pt/STA-ZrO_2 consists of Pt particles that are uniformly distributed across the STA-ZrO_2 surface where the average Pt particle size were found to be less than ~3 nm. Moreover, the Pt/t-ZrO_2 and Pt/S-ZrO_2 catalysts exhibited an increased average size of the Pt particle from ~9 to 11 nm. It has to be noted that the average Pt particle size is within the range. These findings are well-matched with the results of XRD and CO chemisorption.
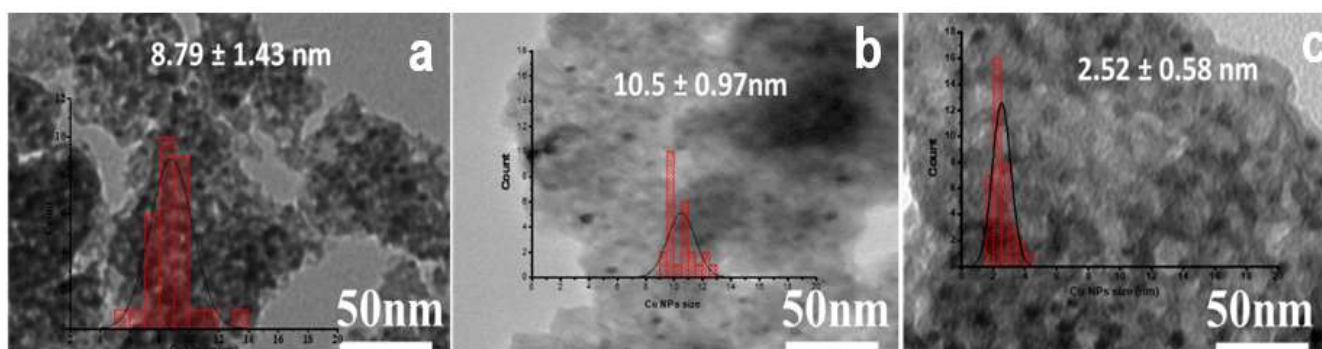
Figure 2. TEM images of various zirconia-based Pt catalysts (**a**) Pt/t-ZrO$_2$, (**b**) Pt/S-ZrO$_2$, and (**c**) Pt/STA-ZrO$_2$.

3.3. BET Surface Area and CO Chemisorption

Table 1 summarizes the textural properties of Pt-loaded t-ZrO$_2$, S-ZrO$_2$, and STA-ZrO$_2$ catalysts and their parent samples. The BET-specific surface area of pure t-ZrO$_2$, S-ZrO$_2$, and STA-ZrO$_2$ samples was 75, 72, and 70 m^2/g. Compared to the parent catalyst support, the supported catalysts had lower BET surface area values because of the presence of Pt, and the activity of all zirconia catalysts was reduced. This was primarily due to Pt metal particles being wholly covered on the surface. Table 1 shows the results of irreversible CO chemisorption on various Pt-loaded ZrO$_2$ samples to evaluate Pt dispersion (percent), metal surface area (m^2/g), and an average particle size (nm). According to the findings, the Pt/STA-ZrO$_2$ catalyst had the highest metal dispersion (19.1%) and metal surface area (51 m^2/g) because of the big pore size and high surface area. Moreover, Pt/t-ZrO$_2$ catalyst has proved to have the smallest amount of metal dispersion (17.6%) and the smallest metal area (39 m^2/g) [32,33].

Table 1. Results of CO uptake, dispersion, metal area, and average particle size of various zirconia-based Pt catalysts.

Samples	BET Surface Area (m^2/g)	ICP-AES	CO Uptake (ml/g)	Pt Metal Area (m^2/g)	Dispersion (%)	Particle's Size (nm)
Pt/t-ZrO$_2$	56	1.80	0.15	39	17.6	5.1
Pt/S-ZrO$_2$	55	1.78	0.20	45	18.3	4.8
Pt/STA-ZrO$_2$	51	1.79	0.25	49	19.1	4.5

3.4. FT-IR Spectroscopy of Pyridine Adsorption Studies

The pyridine adsorption process was followed by an FTIR to determine the several types of acid sites on the catalyst, including Lewis acid (L) and Brønsted acid (B). All of the samples contained absorption bands at 1445–1460 cm^{-1} and 1540–1548 cm^{-1}, respectively, are indicative of L sites (coordinated pyridine) and B sites (protonated pyridine), as shown in Figure 3. Another IR absorption band was also discovered between 1490 and 1500 cm^{-1}, which is related to both L and B sites. When Pt was impregnated on t-ZrO$_2$, an intriguing occurrence was seen. B sites and B+L sites increased along with the Pt content, and at the same time, L sites decreased. Additionally, when Pt is placed onto S-ZrO$_2$, the concentration of L and B sites increases. This may be the result of Pt^{+2} interacting with the surface of S-ZrO$_2$. In comparison to other catalysts, the Pt/STA-ZrO$_2$ sample showed the highest number of L sites and a moderately greater number of B sites, as shown in Figure 3.
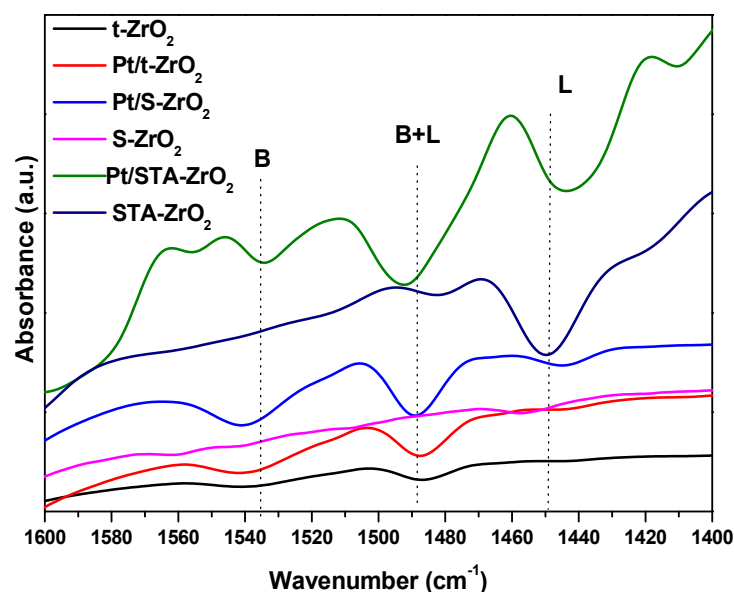
Figure 3. Pyridine FTIR spectra profiles of ZrO_2-based catalysts.

3.5. Catalyst Screening

Table 2 shows the performance of tetragonal and functionalized zirconia supports and the related Pt-loaded catalysts systems for the esterification of LA to EL at 180 °C in the vapor phase utilizing ethanol as a hydrogen donor/alkylating agent. Because noncatalyzed could not proceed without Pt, no GVL synthesis occurred. Using several functionalized zirconia-supported Pt catalysts, the esterification of LA to EL was generally distinct. Among all the catalytic systems, STA-functionalized ZrO_2 considerably enhanced LA conversion. The Pt/STA-ZrO_2 catalyst has been shown to have the best selectivity to EL (92%) and the highest LA conversion (89%). Other minor by-products such as GVL and VA were also detected; however, when Pt was loaded on S-ZrO_2, the LA conversion was 85% and EL selectivity was 81%. This could be because STA-ZrO_2 has a lower acidic strength. The benefit of active Pt sites was not limited to EL production from LA.

Table 2. Effect of zirconia oxide phases of Pt catalysts over LA esterification.

Catalysts	LA Conv. (%)	EL	GVL	VA	Others
Pt/t-ZrO_2	81	85	8	5	2
Pt/S-ZrO_2	85	81	10	6	3
Pt/STA-ZrO_2	89	92	3	3	2

Reaction conditions: LA: ethanol mole ratio-l:20, temperature-240 °C, feed flow-0.5 mL/h, and N_2 flow-30 mL/h.

The Pt/STA-ZrO_2 catalyst was the best catalyst for EL production because it had the highest conversion (89%) and EL production rates. Combined with the above characterization, we conclude that the high catalytic performance of STA-ZrO_2 may be due to its larger number of acidic sites and of active Pt sites covered on the catalyst's surface.

3.5.1. Effect of LA Concentration

The LA concentration could be crucial to the catalytic performance of Pt/STA-ZrO_2 for LA converted to EL production, and the results are shown in Figure 4. There was drop in LA conversion from 92% to 74% with EL selectivity almost constant while LA concentration increased from 20 to 50 wt./wt.%. This could have been due to a limited number of Pt active sites on the surface of STA-ZrO_2.
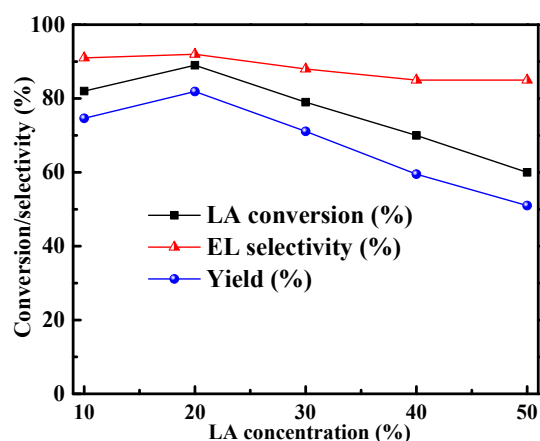
Figure 4. Effect of LA concentration concerning EL selectivity over Pt/STA-ZrO$_2$ catalyst.

3.5.2. Effect of Reaction Temperature

The temperature effect also has importance for catalytic performance [14,34]. Hence, the catalytic systems were investigated at different reaction temperatures between 160 °C to 280 °C to optimize the reaction temperature for the esterification of LA with ethanol. The results as shown in Figure 5. The product distribution changes with the reaction temperature with the complete conversion of LA. At 160 °C, the LA conversion was 35%, and EL selectivity was 30%. As the reaction temperature increased from 160 to 240 °C, the LA conversion and selectivity to EL increased to 89% and 92%. A gradual decrease in the selectivity towards EL was observed beyond 260 °C. In contrast, the selectivity of by-products increases significantly, indicating that the temperature plays a key role in producing EL from LA. Therefore, the Pt/STA-ZrO$_2$ catalyst optimized a reaction temperature to perform the esterification of LA to EL at 240 °C.
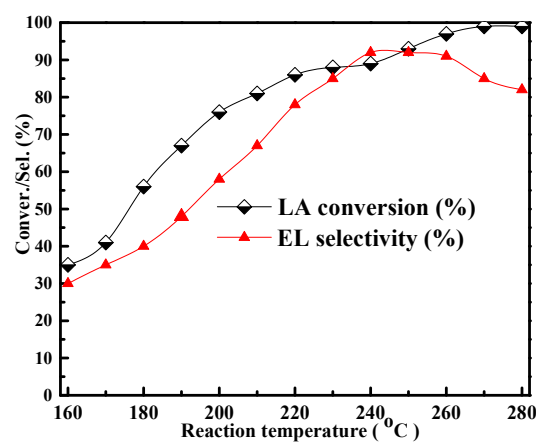

Figure 5. Effect of temperature on esterification of LA with ethanol over Pt/STA-ZrO$_2$ catalyst.

3.5.3. Effect of Hydrogen-Donor

Because the H$_2$ donor (or solvent) is thought to be important in the esterification of LA to ALs, various alcohols such as MeOH, EtOH, 1-Propanol, and 2-Butanol have been employed in the esterification of LA, utilizing the best-optimized catalyst, Pt/STA-ZrO$_2$. As shown in Table 3, each type of alcohol might provide an H-atom for the esterification of LA, whereas the corresponding alcohol structure should affect LA conversion and GVL selectivity. The LA conversion of 81% and the methyl levulinate (ML) selectivity of 85% were obtained when the reaction was carried out in MeOH. Among all the solvents, EtOH is the best solvent for achieving maximal LA conversion and EL selectivity of 89% and 92%, respectively, among all the solvents. The rest of the H$_2$ donor or solvent results are presented in Table 3.

Table 3. ALs synthesis from esterification of LA with various alcohols over Pt/STA-ZrO$_2$ catalyst.

| H-Donor	LA Conversion (%)	Esterification of LA (%)	Resulted Product
MeOH	81	85	Methyl levulinate (ML)
EtOH	89	92	Ethyl levulinate (EL)
PrOH	72	81	Propyl levulinate (PL)
BuOH	71	80	Butyl levulinate (BL)

3.5.4. Effect of Ethanol Amount

The influence of ethanol from 10 mL to 25 mL on the esterification of LA with ethanol (l:10 to l:25) to yield EL using the Pt/STA-ZrO$_2$ catalyst was investigated, and the results are demonstrated in Figure 6. EL selectivity reached 60% with a complete conversion of LA in 10 mL of ethanol. EL self-reacted and formed oligomeric products, which slowed down LA esterification. When the reaction was carried out with LA with 10 mL of ethanol, the EL selectivity reached 60% with the complete conversion of LA in 10 mL ethanol, and it went through self-reaction and forms oligomeric products, which slowed down the LA esterification. When the ethanol volume was 20 mL, the selectivity of EL increased to 92%, and no considerable change was observed. Therefore, the high dilution with ethanol to LA was necessary to perform the esterification reaction.
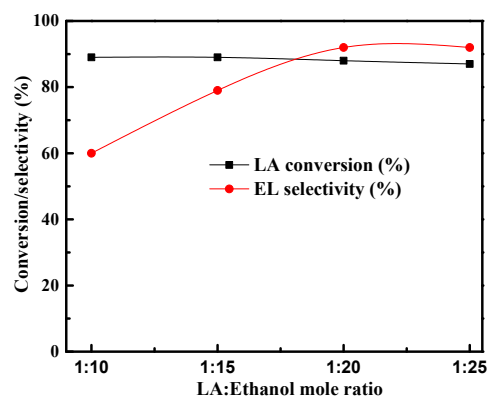
Figure 6. Mole ratio (LA to ethanol) effect using Pt/STA-ZrO$_2$ catalyst. Reaction conditions: temperature-240 °C, feed flow-0.5 mL/h, and N$_2$ flow-30 mL/h.

3.5.5. Effect of Catalyst Amount

The effect of the catalyst amount of the Pt/STA-ZrO$_2$ catalyst has been studied under similar reaction conditions over the esterification of LA with ethanol, as shown in Figure 7. These results show that the conversion of LA and selectivity of EL increases from 51 to 89 and 41% to 92% with the increase in the catalyst amount from 0.1 g to 0.5 g and remains constant beyond 0.5 g. This might be due to the accessibility of many acidic sites for converting the reactants, which leads to increased EL production.
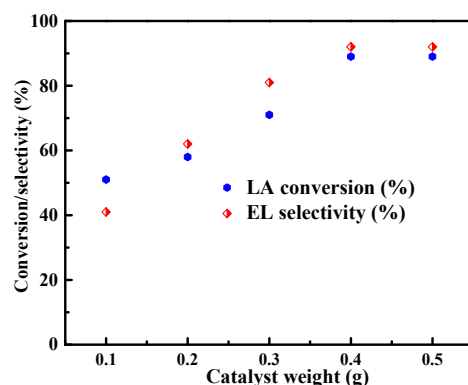
Figure 7. Effect of Pt/STA-ZrO$_2$ catalyst weight on esterification of LA with ethanol.

3.5.6. Time on Stream (TOS)

The esterification of LA to EL has a reaction streaming effect. As demonstrated in Figure 8, when reaction streaming was increased, the LA conversion was enhanced to 89% after 3 h. After that, it stayed stable until 10 h and 11 h, when it finally dropped to 60%. To begin, 87% selectivity to EL is attained in the first hour, which increases to 92% after 3 h of reaction streaming and then drops to 68% after 11 h.
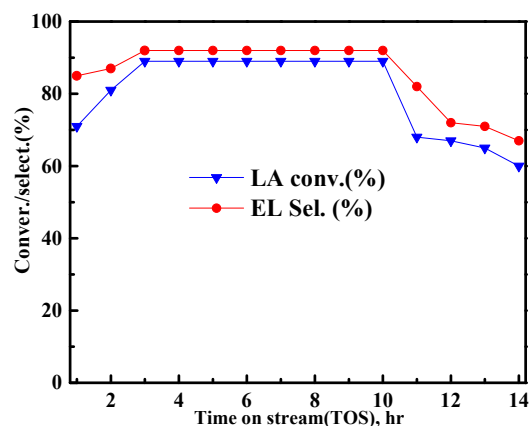

Figure 8. Time on stream studies of Pt/STA-ZrO$_2$ catalyst on LA esterification.

4. Conclusions

In summary, a co-precipitation method was utilized to synthesis platinum (Pt) nanoparticles immobilized on functionalized zirconia, namely, Pt/t-ZrO$_2$, Pt/S-ZrO$_2$, and Pt/STA-ZrO$_2$. Various techniques thoroughly characterize these catalysts: BET, XRD, CO adsorptive decomposition, and TEM, and these results were well correlated with catalytic activity for ALs synthesis. Under optimum reaction conditions (240 °C, 0.5 MPa), 89% conversion of LA with 92% selectivity to EL was obtained over the Pt/STA-ZrO$_2$ catalyst. This catalyst was also stable up to 11 h without much deactivation, and a decrease in selectivity. As compared to Pt/t-ZrO$_2$ and Pt/S-ZrO$_2$, Pt/STA-ZrO$_2$ has the highest number of acidity sites (212 μmol g^{-1}), largest Pt surface area (49 m^2 g^{-1}), and better dispersion (19.1%) of Pt active species over STA-ZrO$_2$; these are the primary reasons for the best catalytic performance activity of the alkyl levulinate biofuels production.

Author Contributions: R.P. and R.B.: conceptualization, methodology, supervision, writing, and editing-original draft; N.M., H.M., R.G., V.P., A.B.R. and A.M.A.: data curation and results analysis; and funding acquisition N.A.-Q. All authors have read and agreed to the published version of the manuscript.

Institutional Review Board Statement: Not applicable.

Informed Consent Statement: Not applicable.

Data Availability Statement: Data are contained within the article.

Conflicts of Interest: The authors declare no conflict of interest.

References

1. Cherubini, F. The Biorefinery Concept: Using Biomass Instead of Oil for Producing Energy and Chemicals. *Energy Convers. Manag.* **2010**, *51*, 1412–1421. [CrossRef]
2. Braden, D.J.; Henao, C.A.; Heltzel, J.; Maravelias, C.C.; Dumesic, J.A. Production of Liquid Hydrocarbon Fuels by Catalytic Conversion of Biomass-Derived Levulinic Acid. *Green Chem.* **2011**, *13*, 1755. [CrossRef]
3. Bozell, J.J.; Petersen, G.R. Technology Development for the Production of Biobased Products from Biorefinery Carbohydrates—The US Department of Energy's "Top 10" Revisited. *Green Chem.* **2010**, *12*, 539. [CrossRef]
4. Xu, W.; Chen, X.; Guo, H.; Li, H.; Zhang, H.; Xiong, L.; Chen, X. Conversion of Levulinic Acid to Valuable Chemicals: A Review. *J. Chem. Technol. Biotechnol.* **2021**, *96*, 3009–3024. [CrossRef]
5. Di Menno Di Bucchianico, D.; Wang, Y.; Buvat, J.-C.; Pan, Y.; Casson Moreno, V.; Leveneur, S. Production of Levulinic Acid and Alkyl Levulinates: A Process Insight. *Green Chem.* **2022**, *24*, 614–646. [CrossRef]
6. Démolis, A.; Essayem, N.; Rataboul, F. Synthesis and Applications of Alkyl Levulinates. *ACS Sustain. Chem. Eng.* **2014**, *2*, 1338–1352. [CrossRef]
7. Sah, P.P.T.; Ma, S.-Y. Levulinic acid and its esters. *J. Am. Chem. Soc.* **1930**, *52*, 4880–4883. [CrossRef]
8. Ahmad, E.; Khan, T.S.; Alam, M.I.; Pant, K.K.; Ali Haider, M. Understanding Reaction Kinetics, Deprotonation and Solvation of Brønsted Acidic Protons in Heteropolyacid Catalyzed Synthesis of Biorenewable Alkyl Levulinates. *Chem. Eng. J.* **2020**, *400*, 125916. [CrossRef]
9. Nandiwale, K.Y.; Niphadkar, P.S.; Deshpande, S.S.; Bokade, V.V. Esterification of Renewable Levulinic Acid to Ethyl Levulinate Biodiesel Catalyzed by Highly Active and Reusable Desilicated H-ZSM-5. *J. Chem. Technol. Biotechnol.* **2014**, *89*, 1507–1515. [CrossRef]
10. Hengne, A.M.; Kamble, S.B.; Rode, C.V. Single Pot Conversion of Furfuryl Alcohol to Levulinic Esters and γ-Valerolactone in the Presence of Sulfonic Acid Functionalized ILs and Metal Catalysts. *Green Chem.* **2013**, *15*, 2540. [CrossRef]
11. Ganji, P.; Roy, S. Conversion of Levulinic Acid to Ethyl Levulinate Using Tin Modified Silicotungstic Acid Supported on Ta_2O_5. *Catal. Commun.* **2020**, *134*, 105864. [CrossRef]
12. Pothu, R.; Gundeboyina, R.; Boddula, R.; Perugopu, V.; Ma, J. Recent Advances in Biomass-Derived Platform Chemicals to Valeric Acid Synthesis. *New J. Chem.* **2022**, *46*, 5907–5921. [CrossRef]
13. Tabassum, N.; Pothu, R.; Pattnaik, A.; Boddula, R.; Balla, P.; Gundeboyina, R.; Challa, P.; Rajesh, R.; Perugopu, V.; Mameda, N.; et al. Heterogeneous Catalysts for Conversion of Biodiesel-Waste Glycerol into High-Added-Value Chemicals. *Catalysts* **2022**, *12*, 767. [CrossRef]
14. Pothu, R.; Challa, P.; Rajesh, R.; Boddula, R.; Balla, P.; Ravi, B.; Perugopu, V.; Radwan, A.B.; Abdullah, A.M.; Qahtani, N.A. Selective Hydrogenation of γ-Valerolactone to 2-Methyltetrahydrofuran Biofuel over Silica Supported Copper Catalysts in the Vapour-Phase. *Nanomaterials* **2022**, *12*, 3414. [CrossRef]
15. Zhang, W.; Wang, Z.; Huang, J.; Jiang, Y. Zirconia-Based Solid Acid Catalysts for Biomass Conversion. *Energy Fuels* **2021**, *35*, 9209–9227. [CrossRef]
16. Masudi, A.; Muraza, O. Zirconia-Based Nanocatalysts in Heavy Oil Upgrading: A Mini Review. *Energy Fuels* **2018**, *32*, 2840–2854. [CrossRef]
17. Li, X.; Nagaoka, K.; Simon, L.; Olindo, R.; Lercher, J. Mechanism of Butane Skeletal Isomerization on Sulfated Zirconia. *J. Catal.* **2005**, *232*, 456–466. [CrossRef]
18. Luo, Z.; Wang, Y.; He, M.; Zhao, C. Precise Oxygen Scission of Lignin Derived Aryl Ethers to Quantitatively Produce Aromatic Hydrocarbons in Water. *Green Chem.* **2016**, *18*, 433–441. [CrossRef]
19. Zhang, J.; Wu, Z.; Li, X.; Zhang, Y.; Bao, Z.; Bai, L.; Wang, F. Catalytic Cracking of Inedible Oils for the Production of Drop-In Biofuels over a SO_4^{2-}/TiO_2-ZrO_2 Catalyst. *Energy Fuels* **2020**, *34*, 14204–14214. [CrossRef]
20. Joo, J.B.; Vu, A.; Zhang, Q.; Dahl, M.; Gu, M.; Zaera, F.; Yin, Y. A Sulfated ZrO_2 Hollow Nanostructure as an Acid Catalyst in the Dehydration of Fructose to 5-Hydroxymethylfurfural. *ChemSusChem* **2013**, *6*, 2001–2008. [CrossRef]
21. Qu, Y.; Zhao, Y.; Xiong, S.; Wang, C.; Wang, S.; Zhu, L.; Ma, L. Conversion of Glucose into 5-Hydroxymethylfurfural and Levulinic Acid Catalyzed by SO_4^{2-}/ZrO_2 in a Biphasic Solvent System. *Energy Fuels* **2020**, *34*, 11041–11049. [CrossRef]
22. Unlu, D.; Ilgen, O.; Hilmioglu, N.D. Biodiesel Additive Ethyl Levulinate Synthesis by Catalytic Membrane: SO_4^{-2}/ZrO_2 Loaded Hydroxyethyl Cellulose. *Chem. Eng. J.* **2016**, *302*, 260–268. [CrossRef]
23. Saravanamurugan, S.; Riisager, A. Solid Acid Catalysed Formation of Ethyl Levulinate and Ethyl Glucopyranoside from Mono- and Disaccharides. *Catal. Commun.* **2012**, *17*, 71–75. [CrossRef]
24. Morales, G.; Osatiashtiani, A.; Hernández, B.; Iglesias, J.; Melero, J.A.; Paniagua, M.; Robert Brown, D.; Granollers, M.; Lee, A.F.; Wilson, K. Conformal Sulfated Zirconia Monolayer Catalysts for the One-Pot Synthesis of Ethyl Levulinate from Glucose. *Chem. Commun.* **2014**, *50*, 11742–11745. [CrossRef]
25. Song, D.; An, S.; Sun, Y.; Guo, Y. Efficient Conversion of Levulinic Acid or Furfuryl Alcohol into Alkyl Levulinates Catalyzed by Heteropoly Acid and ZrO2 Bifunctionalized Organosilica Nanotubes. *J. Catal.* **2016**, *333*, 184–199. [CrossRef]
26. Zhang, Z.; Yuan, H. An Alumina-Coated UiO-66 Nanocrystalline Solid Superacid with High Acid Density as a Catalyst for Ethyl Levulinate Synthesis. *J. Chem. Technol. Biotechnol.* **2020**, *95*, 2930–2942. [CrossRef]
27. Quereshi, S.; Ahmad, E.; Pant, K.K.; Dutta, S. Synthesis and Characterization of Zirconia Supported Silicotungstic Acid for Ethyl Levulinate Production. *Ind. Eng. Chem. Res.* **2019**, *58*, 16045–16054. [CrossRef]

28. Derle, S.N.; Parikh, P.A. Hydrogenation of Levulinic Acid and γ-Valerolactone: Steps towards Biofuels. *Biomass Convers. Biorefin.* **2014**, *4*, 293–299. [CrossRef]

29. Oh, J.; Dash, S.; Lee, H. Selective Conversion of Glycerol to 1,3-Propanediol Using Pt-Sulfated Zirconia. *Green Chem.* **2011**, *13*, 2004–2007. [CrossRef]

30. Fu, J.; Lym, J.; Zheng, W.; Alexopoulos, K.; Mironenko, A.V.; Li, N.; Boscoboinik, J.A.; Su, D.; Weber, R.T.; Vlachos, D.G. C–O Bond Activation Using Ultralow Loading of Noble Metal Catalysts on Moderately Reducible Oxides. *Nat. Catal.* **2020**, *3*, 446–453. [CrossRef]

31. Huy, H.A.; van Man, T.; Tai, H.T. Preparation and Characterization of High-Dispersed Pt/c Nano-Electrocatalysts for Fuel Cell Applications. *Vietnam. J. Sci. Technol.* **2016**, *54*, 472. [CrossRef]

32. Zhu, S.; Qiu, Y.; Zhu, Y.; Hao, S.; Zheng, H.; Li, Y. Hydrogenolysis of Glycerol to 1,3-Propanediol over Bifunctional Catalysts Containing Pt and Heteropolyacids. *Catal. Today* **2013**, *212*, 120–126. [CrossRef]

33. Alsalme, A.M.; Wiper, P.V.; Khimyak, Y.Z.; Kozhevnikova, E.F.; Kozhevnikov, I.V. Solid Acid Catalysts Based on H3PW12O40 Heteropoly Acid: Acid and Catalytic Properties at a Gas-Solid Interface. *J. Catal.* **2010**, *276*, 181–189. [CrossRef]

34. Pothu, R.; Harisekhar, M.; Boddula, R.; Raveendra, G.; Balla, P.; Ravi, B.; Perugopu, V.; Ma, J. Direct Cascade Hydrogenation of Biorenewable Levulinic Acid to Valeric Acid Biofuel Additives over Metal (M = Nb, Ti, and Zr) Supported SBA-15 Catalysts. *Mater. Sci. Energy Technol.* **2022**, *5*, 391–398. [CrossRef]